

# Effects of Hydrocarbon Liquid Feed on Particle Temperature Rise During Gas Phase Polymerization of Polyethylene

*K.K. Botros, G. Price, Fluid Dynamics Group*

*V. Ker, Y. Jiang, and S. K. Goyal, Gas Phase PE Process R&D Group*

*NOVA Chemicals Research & Technology Centre, Calgary, Alberta, Canada.*

*Prepared for presentation at the AIChE Annual Meeting, Particle Technology Forum, November 7-12, 2004, Austin, Texas. AIChE shall not be responsible for statements or opinions in papers or printed in its publications.*

## ABSTRACT

In the fluidized bed gas phase polymerization of polyethylene (PE), the heat generated by the exothermic polymerization process is dissipated into the gas mixture flowing past the polymer particles. The polymer particle temperature is determined by the extent of convective heat transfer and other mechanisms of heat removal. In addition to the heat removal by convective heat transfer, liquid hydrocarbon (HC) is often injected into the reactor to further remove heat by evaporation but without partaking in the reaction. The effects of adding this liquid HC on the particle surface temperature have been investigated numerically by means of a one-dimensional polar model. Results indicate that the primary mechanism for removal of the heat of polymerization from the particles is by means of convective heat transfer to the bulk gas, which amounts to 99.5% removal of total heat of polymerization. The PE particle temperature rises only by 1- 2 °C above the surrounding bed gas mixture. The addition of liquid HC to the feed, however, has a pronounced effect on controlling the reactor gas temperature as most of this liquid is evaporated to the gaseous phase before it reaches the polymer particles. To state it clearly, heat of polymerization is transferred from the particles to the reactor bulk gas predominantly by convection, and part of this heat is subsequently absorbed by evaporation of the fresh liquid HC in the feed. Comparison with detailed Computational Fluid Dynamic (CFD) model of polymerization in a generic gas phase reactor has also been conducted. The results confirm that the particle temperature rise above the reactor gas temperature is consistent with the one-dimensional model. However, local gas temperature variations are present in the reactor due to the unsteady gas-solid hydrodynamics. Hence, there are some zones that are a few degrees hotter/colder than the bulk reactor temperature with corresponding increase/decrease in particle temperature in these zones.

## NOMENCLATURE:

- $A_o$  = constant in the kinetic profile.
- $C_f$  = fraction of the liquid feed that reaches the polymer particle (=1, when all the fresh liquid feed reaches all polymer particles, and = 0, if no fresh liquid reaches the polymer particles).
- $D$  = final diameter of the particle at end of polymerization reaction (=2R).
- $c$  = specific heat of polymer.
- $k$  = thermal conductivity of polymer.
- $c_g$  = specific heat of the gas mixture.
- $\dot{G}(t)$  = heat liberation due to polymerization per unit volume of the polymer particle.

|           |   |  |
|-----------|---|--|
| $h$       | = | heat transfer coefficient between particle surface and gas mixture.  |
| $k_g$     | = | thermal conductivity of the gas mixture.   |
| $m_f(t)$  | = | mass of liquid film on one polymer particle at time (t).   |
| $m_d(t)$  | = | mass of fresh liquid added to the polymer particle at time (t).  |
| $NP$      | = | number of polymer particles per gm of catalyst.  |
| $Nu$      | = | Nusselt number ( $Nu = h D/k$ ).   |
| $Pr$      | = | Prandtl number of the gas mixture ( $Pr = c_g \cdot \mu_g / k_g$ ).  |
| $P(t)$    | = | instantaneous polymer production per gm of catalyst.   |
| $\hat{P}$ | = | productivity per gm of catalyst after 2 hours.   |
| $Q_p$     | = | heat of polymerization per unit mass of polymer.   |
| $r$       | = | radial dimension of a spherical polymer particle.  |
| $R$       | = | final radius of the polymer particle at end of polymerization reaction.  |
| $Re$      | = | Reynolds number of the relative flow around the polymer particle, based on its diameter and slip velocity between the gas stream and the polymer particle. |
| $S$       | = | monomer consumption (kinetic profile) in standard liters per minute (SLPM).  |
| $\hat{S}$ | = | integral of the entire kinetic profile over 2 hours.   |
| $t$       | = | time.  |
| $T$       | = | temperature.   |
| $T_i$     | = | fresh feed temperature.  |
| $T_o$     | = | reactor gas temperature.   |
| $V$       | = | polymer particle volume.   |
| $V_r$     | = | slip (relative) velocity between polymer particle and gas.   |
| $x_L$     | = | ratio of liquid feed to polymer production.  |

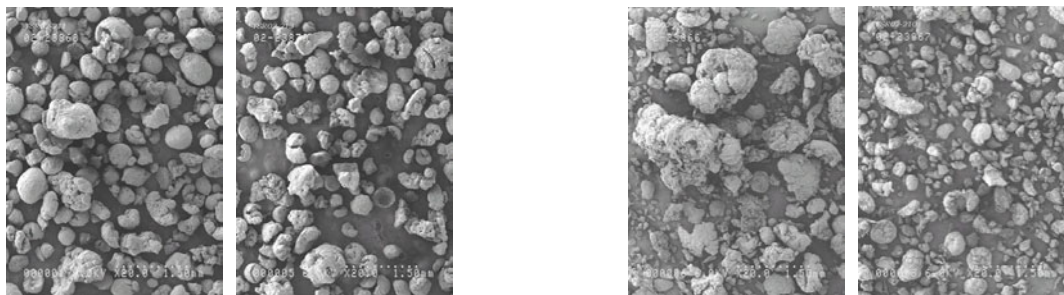
Greek Letters:

|          |   |   |
|----------|---|---|
| $\rho$   | = | effective density of the polymer particle = $\rho_p (1 - \phi)$ . |
| $\rho_p$ | = | polymer density.  |
| $\phi$   | = | porosity of the polymer particles.                                |
| $\alpha$ | = | thermal diffusivity of the polymer particle ( $k/\rho c$ ).       |
| $\mu_g$  | = | dynamic viscosity of the gas mixture.                             |

## 1.0 INTRODUCTION

Performance of new catalysts used in manufacturing polyethylene in fluidized bed reactors is typically evaluated by three key parameters: catalyst productivity, resin morphology and product performance. Higher catalyst productivity is desired to reduce the catalyst cost. Morphology of the resins has to be such that the particles do not fragment into smaller ones during polymerization thus producing fines in the reactor. As the catalyst productivity increases, the amount of heat generated within each particle also increases due to exothermic nature of the polymerization reaction. If this heat of reaction is not removed efficiently from the particles, the temperature of the particles will rise. Depending on the extent of the temperature rise, the particles may fragment into smaller particles (due to rapid uncontrolled growth of particles) or they may melt causing several particles to stick together to form agglomerates. These situations are undesirable for the operation of a gas phase fluidized bed polymerization process.

In addition to the overall catalyst productivity (amount of heat generated within each particle), the rate at which polymerization occurs also appears to be important in controlling the particle temperature and thus the resin morphology. The rate of polymerization is manifested by the kinetic profile for the catalyst during the course of polymerization. During performance evaluation of two new high productivity polyethylene catalysts on a small-scale gas phase reactor, it was found that the resins produced with the new catalysts had a significant amount of fines (small particles) and/or some agglomerated particles. However, when a liquid hydrocarbon (HC) was added to the reactor, the catalyst productivity and/or the resin morphology improved significantly. The effect of the liquid HC was different depending on resin density. Scanning Electron Microscope (SEM) pictures of the resins taken from polymerization experiments with and without liquid HC in the reactor for the two new catalyst formulations are shown in Fig. 1. These pictures clearly exemplify the importance of liquid HC in improving particle morphology.



a) Resin with Liquid HC in the Reactor

b) Resin without Liquid HC in the Reactor

**Figure 1: Effect of Liquid HC in Reactor on Resin Morphology.**

A possibility for the apparent improvement in the polymer particle morphology could arise from the change in the mechanism of heat removal from the particles that could result in moderating the rate of initial particle growth by reducing temperature excursions in the polymer particles especially in high productivity catalysts. It was believed that high initial activity surges could cause the particles to expand too fast leading to fragmentation, high fines and irregular shaped particles. Additionally, liquid HC in the feed, when in contact with the polymer, is thought to be absorbed and swell the polymer particles much more than a gaseous feed thus allowing easier access of monomer to the active sites and in so doing increasing the catalyst productivity. The swelling of polymer by liquid HC could also affect its elastic properties, thus reducing particle fragmentation and improving resin morphology.

In order to understand whether the improved resin morphology with liquid HC was due to reduction in particle temperature excursions or due to other mechanisms such as swelling of the polymer, a numerical investigation was carried out on a generic gas phase fluidized bed reactor. This generic reactor was comprised of a continuous recycle system with a cooler and a fresh feed of monomer, comonomer and make-up liquid HC, as shown in Fig. 2. In this generic reactor, the primary means of removing the heat of polymerization is by recycling the gaseous mixture around the reactor through an external cooler which provides the main heat removal element in the process. Since cooler duties are generally limited, the amount of recycling vs. the amount of polymer produced is generally in the order of 30 to 50 times; hence the conversion rate per pass is generally very low (e.g. 2-3%). Clearly, the available thermal capacity of the cooler limits the production rates of polymers from a given reactor. In order to increase the production rates, additional cooling can be realized by injecting a non-reactive liquid HC agent to the inlet stream, which upon vaporization in the reactor removes part of the polymerization

heat. The evaporated liquid HC is carried over to the recycle stream, and is subsequently cooled and condensed in the cooler and re-injected back into the reactor as liquid HC for further heat removal.

The main objective of the present work is to answer this question: does the addition of liquid HC change the mechanism of heat removal from the PE particles during polymerization such that it affects particle surface temperature and hence morphology? Direct measurements of particle temperature are difficult and impractical. Pater et al. [1] have recently developed an optical method to measure particle surface temperature using an infrared imaging technique. However, their method is not really non-intrusive as the particle remains in contact with a glass surface in a stagnant gas mini-reactor. Therefore, a numerical analysis was pursued in the present investigation, where a transient one-dimensional heat transfer model in the spherical coordinate system of one particle has been developed for this purpose. The model accounts for particle growth but not for particle breakage or agglomeration, similar to the work in [2,3,4], and assumes that monomer diffusion into the particle is instantaneous and uniform. Two different reaction kinetics schemes exemplified by slow and fast decaying catalyst activities were investigated. Comparison with detailed Computational Fluid Dynamic (CFD) model of polymerization in this generic reactor has also been conducted.

## 2.0 ONE DIMENSIONAL GOVERNING EQUATIONS

As mentioned above, in the gas phase fluidized bed process, ethylene and co-monomers polymerize around solid catalyst particles. Most of the heat generated by this exothermic process is dissipated into the gas mixture flowing past the particle, but some heat is retained by the PE particle as it forms and grows. The retained heat within the PE particle gives rise to a higher polymer temperature than that of the surrounding gas mixture. Thus, it is essential to remove as much of the heat of polymerization as possible from the growing PE particles over the course of the polymerization process.

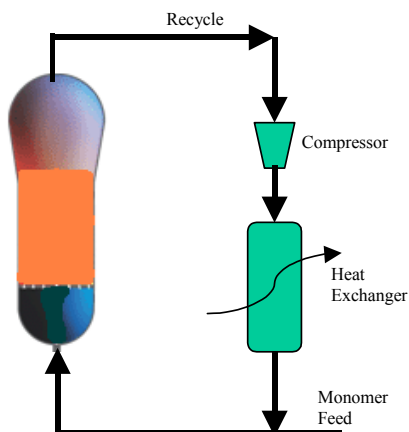


**Figure 2: Schematic of the Generic Reactor Used in the present Study.**

A thermal heat conduction/convection model has been developed to assess the heat transfer from a growing PE particle. A portion of the liquid HC fed to the reactor is assumed to come into contact with the polymer particle during polymerization and is allowed to extract some of the heat liberated via evaporation. Not all of the liquid feed that comes into contact with PE particles will evaporate depending on the particle surface temperature at the time of contact. The remaining un-evaporated portion would be absorbed by the particle and would have to be removed in the polymer discharge system. In the present

model, this remaining liquid is assumed to form a liquid film of a certain thickness on the surface of the PE particle for quantification purpose. The main assumptions of model are:

- Monomer diffusion into the particle is instantaneous and uniform.
- Polymerization reaction kinetics and hence particle growth that follows the kinetic profile are known.
- The model focuses on the heat removal mechanism during polymerization and not the polymer particle morphology; hence particle growth was assumed mono-dispersed without breakage or agglomeration during polymerization.
- Polymer-catalyst phase is treated as a pseudo-homogeneous porous medium with an effective density.
- Liquid film on particle surface has negligible thermal resistance.

Assuming polymerization is taking place uniformly in the spherical particle, the governing equation for the temperature distribution within the particle due to heat liberated by polymerization is given by:

$$\rho c \left( \frac{\partial T}{\partial t} \right) = k \frac{1}{r^2} \frac{\partial}{\partial r} \left[ r^2 \frac{\partial T}{\partial r} \right] + G(t) \quad (1)$$

where the outer radius (R) of the sphere is subject to growth due to polymerization, i.e.:

$$R = R(t) \quad (2)$$

Initial Condition:

$$T = T_i \quad 0 \leq r \leq R \quad (3)$$

Boundary Conditions:

$$-k \, 4\pi R^2 \left( \frac{\partial T}{\partial r} \right)_R \delta t = QE + h \, 4\pi R^2 (T_R - T_0) \delta t \quad (4)$$

$$\left( \frac{\partial T}{\partial r} \right) = 0 \quad \text{at } r = 0, \text{ all time} \quad (5)$$

The second term on the right-hand-side of equation (4) represents the heat transfer by convection to the gas phase, while the first term (QE) represents the heat of evaporation composed of two parts (illustrated in the schematic of Fig. 3):

- The first part is the heat required to evaporate the portion of the liquid film that has already accumulated on the PE particle over time (QE<sub>i</sub>), from temperature T(t) to T(t+δt).
- The second part is the heat required to evaporate the fresh liquid (per particle) that comes into contact with the particle (QE<sub>ii</sub>) from the fresh feed at temperature T<sub>i</sub> to the current surface temperature of the particle T(R, t).

Hence

$$QE = QE_i + QE_{ii} \quad (6)$$

The convective heat transfer coefficient to the surrounding gas mixture may be determined from Ranz-Marshall correlation [5], which is expressed as:

$$\frac{hD}{k_g} = 2.0 + 0.6 \text{Re}^{1/2} \text{Pr}^{1/3} \quad (7)$$

Based on the experimental evidence, Kiel et al. [6] argued that the actual heat transfer coefficient in a gas-solid particle under trickle flow conditions is around 30-35% of that predicted by Ranz-Marshall correlation. Gunn [7], however, disputed this argument and argued that the Nusselt number cannot be below a value of 2.0 in the extreme low Reynolds number as the analytical asymptotic value should be equal to exactly 2.0 for a sphere in a stagnant conducting medium (see, e.g. ref [8]).

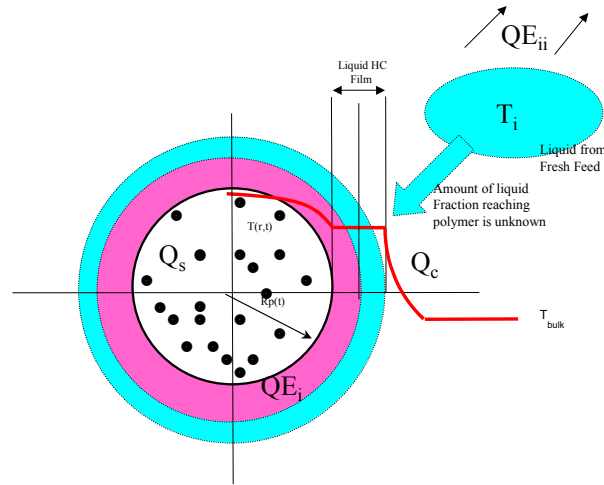


**Figure 3: Heat Balance of a Polymer Particle with Liquid HC Feed.**

Equations (1), (4) and (6) imply that the heat liberated from polymerization per particle ( $Q$ ) is distributed to three places, namely:

- i) Heat retained in the polymer particle in the form of *sensible* heat ( $Q_s$ ), resulting in an increase in its temperature in each time step and distributed according to the conduction equation (1) above.
- ii) Heat of *evaporation* required to evaporate a portion of the liquid film around one spherical particle ( $QE_i$ ) from temperature  $T(t)$  to  $T(t+\delta t)$  and that required to evaporate the additional liquid added to each particle ( $QE_{ii}$ ) from the fresh feed temperature  $T_i$  to the current surface temperature of the particle  $T(r, t)$ .
- iii) Heat dissipated by *convection* to the reactor bulk gas ( $Q_c$ ).

Hence:

$$Q = Q_s + QE_i + QE_{ii} + Q_c \quad (8)$$

### 3.0 SOLUTION TECHNIQUE

Equation (1) was numerically solved using the Crank-Nicolson method which is stable for all values of  $\delta r$  and  $\delta t$ , with truncation error in the order of  $(\delta t)^2 + (\delta r)^2$ . In the present study, the value of  $(\alpha \delta t / \delta r^2)$  was maintained around 0.5 to further guarantee stability of the solution. However, in transient heat transfer problems governed by conduction, the time is scaled with a dimensionless number called the Fourier number defined as:

$$Fourier\ number = \frac{t\alpha}{R^2} = \frac{t}{\tau} \quad (9)$$

where  $\tau$  is the time scale associated with the geometrical dimension of the problem in hand and the thermal diffusivity of the conductive material  $\alpha$ .

In the present problem, the highest particle surface temperature is attained within the first 5 seconds of reaction, and the particle size at this time is only in the order of 100 microns ( $R = 50$  microns). Since  $\alpha = 2.08 \text{ e-}07$ , the time constant  $\tau$  would be equal to 12 milliseconds. This implies that a thermal wave takes in the order of 12 milliseconds to travel one radius of the spherical particle. Steady state may be attained after say  $10\tau$ . Therefore, transient heat transfer by conduction in the polymer particle can only be manifested within the first 120 milliseconds of any change in the boundary condition. According to kinetic profiles of polymerization, the highest gradient of ethylene conversion occurs in the first 5 minutes (300 seconds). Therefore, polymerization is deemed to be very slow compared to the time scale  $\tau$  of the problem. Hence, it is anticipated that the solution of equation (1) would reflect a quasi-steady state solution following the shape of the kinetic profile of polymerization.

Following this logic, one can utilize the heat balance equation (8) and solve it at each time step ( $\delta t$ ). Equation (8) can then be expressed based on one gram of catalyst and known final productivity after 2 hours (in terms grams of polymer produced per gram of catalyst), and final polymer density and particle porosity. Hence, the heat liberated per particle ( $\delta Q$ ) is:

$$\delta Q = \frac{\delta P \cdot Q_p}{NP} = \frac{\delta S \cdot \hat{P} \cdot Q_p}{NP} \quad (10)$$

And, the polymer production per particle at any given time is given by:

$$P(t) = \frac{\hat{P}}{NP} \int_0^t S dt \quad (11)$$

The sensible heat gained per particle ( $\delta Q_s$ ) is:

$$\delta Q_s = \rho c V [T(t + \delta t) - T(t)] \quad (12)$$

where,  $V(t)$  is the time varying volume of one particle determined from the following equation:

$$V(t) = \frac{P(t)}{\rho NP} \quad \text{and} \quad R(t) = \left[ \frac{3V(t)}{4\pi} \right]^{(1/3)} \quad (13)$$

The heat of evaporation of the liquid film present on the particle ( $\delta QE_i$ ) is:

$$\delta QE_i = m_f(t) [q_i(t + \delta t) - q_i(t)] \quad (14)$$

The heat of evaporation of fresh liquid feed contacting one particle ( $\delta QE_{ii}$ ) is:

$$\delta QE_{ii} = C_f m_d(t) [q_{ii}(T(t))] \quad (15)$$

and

$$m_d(t) = \frac{P(t) \cdot x_L}{NP} \quad (16)$$

The heat of convection from particle to reactor bulk gas is:

$$Q_c = h 4\pi R^2 (T_R(t) - T_0) \delta t \quad (17)$$

#### 4.0 SIMULATION PARAMETERS

Four cases corresponding to different liquid feed and production rates were considered as shown in Table 1. Notice that the ratio of liquid feed rate to polymer production rate is 2.5 in Case 2 and 3.5 in Case 3. Obviously, this significant amount of liquid loading cannot remain in the polymer as it discharges out of the gas phase reactor. In fact, it was estimated that the amount of liquid HC that remains in the polymer is around 4-6% (on mass basis). Therefore, the amount of fresh liquid feed reaching the polymer particle, accounted by the coefficient  $C_f$ , is adjusted such that the final results give the same liquid mass fraction as determined by the global mass balance of the generic reactor. When the fresh liquid/gaseous feed mixture is injected into the reactor, most of the liquid is evaporated according to the thermodynamic flash calculation of the mixture under equilibrium. Only a portion of the feed liquid reaches the PE particle. The amount of liquid that would remain in the particle is determined by a subsequent flash calculation of the liquid phase alone at the prevailing particle temperature. The final liquid fraction remaining on the particle from the portion of fresh liquid reaching the particle is shown in Fig. 4.

Figures 5 and 6 show the heat duty to evaporate the fresh liquid reaching the particle, and the same for evaporating any liquid remained in the particle. Table 2 gives relevant data for the reactor conditions, including bulk gas and polyethylene polymer properties. The kinetic profiles are modeled using the ethylene consumption rate shown in Fig. 7 and scaled up to the generic reactor under consideration.



**Table 1: Simulation Parameters for the Four Cases**

|                                       |          | Case 1 | Case 2 | Case 3 | Case 4 |
|---------------------------------------|----------|--------|--------|--------|--------|
| Production Rate                       | kg/hr    | 25000  | 35000  | 45000  | 45000  |
| Rx Temperature                        | C        | 88     | 88     | 88     | 88     |
| Liquid in Feed                        | % (mass) | 0      | 8      | 13     | 13     |
| Feed Temperature                      | C        | 40     | 40     | 33     | 33     |
| Fresh Liquid to Polymer mass ratio    | -        | 0      | 2.50   | 3.50   | 3.50   |
| Liquid fraction reaching particle     | -        | 0      | 0.02   | 0.02   | 100*   |
| Liquid Remained to Polymer mass ratio | -        | 0      | 0.04   | 0.056  | 2.8*   |

\* hypothetical scenario

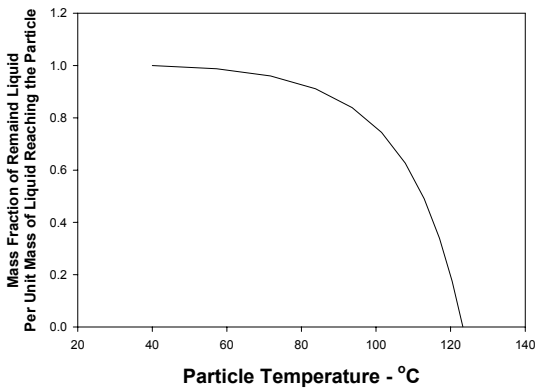


**Figure 4: Mass fraction of the remaining liquid on the particle vs. its surface temperature after flashing the fresh liquid feed at reactor inlet temperature.**

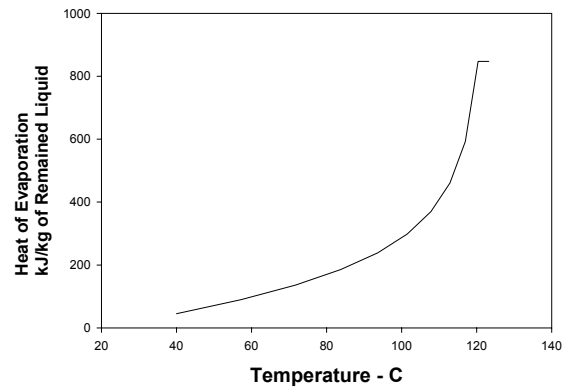


**Figure 6: Heat of evaporation per unit mass of the remaining liquid in the particle vs. particle surface temperature.**

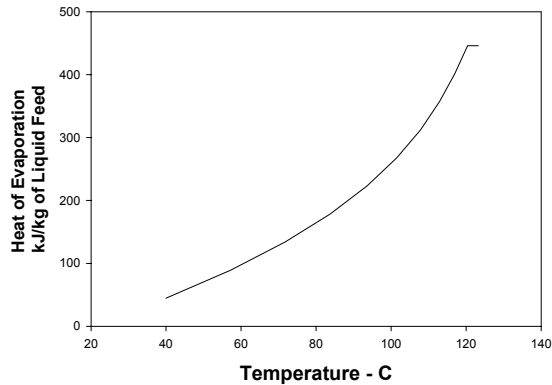


**Figure 5: Heat of evaporation per unit mass of fresh liquid feed to local particle temperature.**

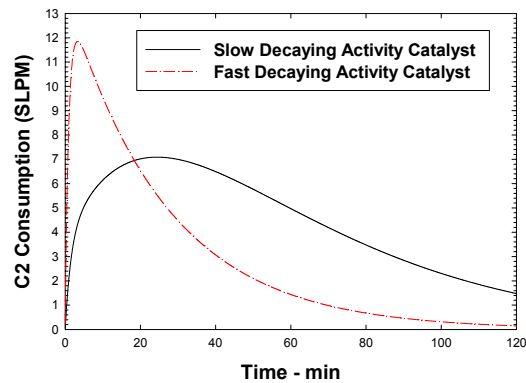


**Figure 7: Examples of slow and fast decaying catalyst activity kinetic profiles.**

The convective heat transfer from the particle surface to the surrounding gas mixture is one of the key mechanisms that controls the evolution of PE particle temperature over time in the reactor. The Ranz-Marshall correlation, Equation (7), indicates that the convective heat transfer coefficient,  $h$ , depends on the particle diameter, the thermal conductivity of the gas phase, the Reynolds number of the relative gas flow past the particle,  $Re = \rho_g V_r D / \mu_g$ , and the Prandtl number for the gas mixture. The Reynolds number depends on the relative slip velocity,  $V_r$ , between the gas and solid phases, which in turn, depends on the reactor internal geometry, local gas velocity and particle diameter. The fluidized bed reactors are inherently unsteady, and the local gas velocity varies from zero to several multiples higher than the operating superficial gas velocity depending on the local solids concentration in the bed. In this case,  $V_r$  can vary from zero to the local gas velocity depending on the particle size and the intensity of the particle concentration. It is impossible to accurately estimate the slip velocity for subsequent calculation of the relative Reynolds number and ultimately accurately estimate the local convective heat transfer coefficient between the gas and solid PE particles.

**Table 2: Relevant Data Used in the Present Study.**

|                                    |   |
|------------------------------------|---|
| Reactor Gas Components             | Ethylene<br>Ethane<br>H2<br>Butene<br>Butane<br>N2<br>Liquid HC |
| Polymer Density (kg/m3)            | 918   |
| Porosity                           | 20%   |
| Effective Particle Density         | 734.40  |
| Heat of Reaction kJ/kg             | 2799.00   |
| Polymer Cp J/kg-K                  | 1306.00   |
| Gas Density kg/m3                  | 25.09   |
| Gas Cp J/kg-K                      | 1744.57   |
| Gas Thermal conductivity J/sec-m-K | 0.03  |
| Gas Viscosity Pa.s                 | 1.39E-05  |

Therefore, a relatively conservative estimate for the average slip velocity ( $V_r = 5$  cm/s) is employed in the present analysis. The rationale for this estimate is that a low slip velocity will yield a lower convective heat transfer coefficient, and hence a conservative prediction of particle temperature. As noted earlier, the Ranz-Marshall correlation is strictly valid only for flow past an isolated particle. The Nusselt number in packed gas-solid beds is generally higher than that for an isolated particle. Gunn [7] examined the heat transfer from particles in fixed and fluidized beds from a theoretical perspective and developed the following correlation which accounts for the porosity of the bed,  $\alpha$  (where  $\alpha = 1.0$  indicates very sparse bed, and  $\alpha = 0.0$  indicates very compact bed):

$$Nu = (7 - 10\alpha + 5\alpha^2)(1 + 0.7 Re^{0.2} Pr^{1/3}) + (1.33 - 2.4\alpha + 1.2\alpha^2) Re^{0.7} Pr^{1/3} \quad (18)$$

This equation gives a higher value for the Nusselt number than the Ranz-Marshall expression. In the present work, Ranz-Marshall correlation was used in the one-dimensional analysis, while Gunn's correlation was used in the CFD simulation.

In order to substantiate the value of the relative slip velocity,  $V_r$ , Computational Fluid Dynamics (CFD) simulation was conducted on the generic fluidized bed reactor. The predicted contours of the relative slip velocity between the gas and the solid phases at two different particle sizes (normalized by the superficial gas velocity  $V_s$ ) are shown on Fig. 8. As expected, the slip velocity between the gas and the solids increases with increasing

particle diameter, i.e.  $V_r$  increases by a factor of two when the particle diameter increases from 100 microns to 673 microns. This agrees with the theory in the limit of very small particles that will tend to move with gas ( $V_r = 0$ ). For small particles, it is estimated that  $V_r/V_s = 0.1-0.2$ . Hence, for  $V_s = 0.4$  m/s, the value of  $V_r = 4-8$  cm/s can be used.

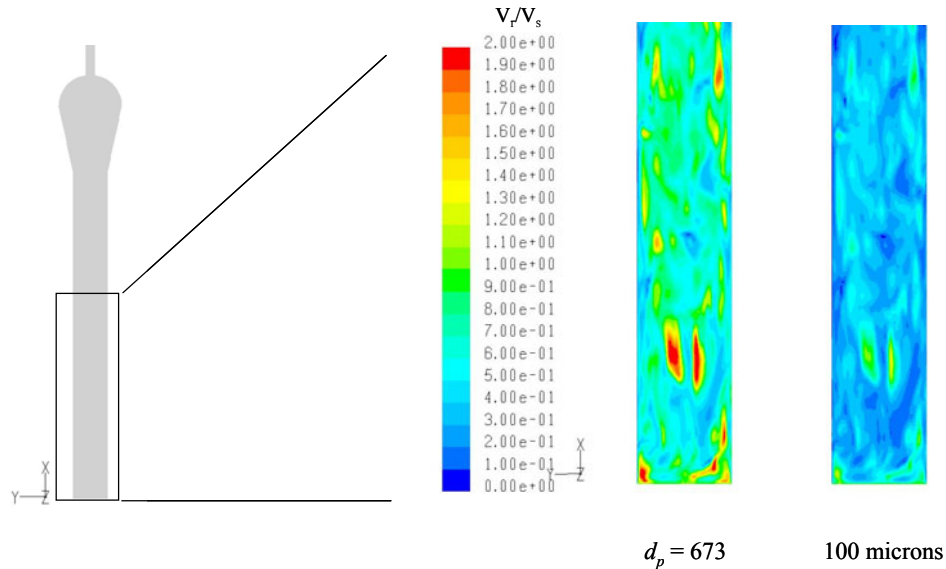


**Figure 8: Contours of relative slip velocity between gas and solid phases (normalized by gas superficial velocity  $V_s = 0.4$  m/s) plotted on a vertical slice plane through the generic reactor.**

## 5.0 RESULTS

### One-Dimensional Analysis:

Numerical simulations were carried out based on the model described in Section 3.0. The results are compared for the two kinetic profiles shown in Fig. 7. Here, we adjusted the  $C_f$  coefficient in equation (15) so as to obtain a 5% remaining liquid HC in the PE particle at the end to the 2 hours of polymerization consistent with the flash calculations data. Figure 9 shows the particle temperature rise above the reactor bulk gas temperature for the two kinetic profiles corresponding to Case 3, where the liquid feed is the highest (13 % by mass). It indicates that the particle temperature rise above the reactor mean bulk temperature is in the order of 1.3 – 2.7 °C, depending on the kinetic profile. Fan et al [8] obtained similar results for different reactor conditions.

The particle size growth over the 2-hour polymerization is depicted in Fig. 10, which indicates a final particle size of 941 microns for the slow decay catalyst activity kinetic profile vs. 782 microns for the fast decay catalyst activity kinetics. The liquid mass fraction remaining in the PE particles is shown in Fig. 11, which was obtained by using  $C_f \cong 0.02$  (i.e. 2% of the liquid feed is reaching the PE particles). This is not surprising considering that the dew point characteristics of the total feed mixture indicates that at a reactor temperature of 88 °C, most of the liquid would have been flashed (evaporated) and very little would reach the PE particles.

The most important finding is shown in Figures 13 and 14, where the relative amounts of heat of polymerization that are removed by the evaporation of the liquid (i.e.,  $QE_i + QE_{ii}$ ) and the heat transfer to the bulk

gas by convection are depicted. It is shown that the heat removed by evaporation of liquid from the PE particle amounts to approximately 0.5% of the total heat generated, while 99.5% or more is actually removed from the particle by convection. Sensible heat retained by the polymer is negligibly small. Clearly, the main mechanism of polymerization heat removal from the PE particles is via convective means to the bulk gas under conditions of zero polymer particle fragmentation.

Further simulations were conducted to substantiate the above observations. Figure 15 compares results of the four cases given in Table 1 for different liquid loadings. Case 4 is the same as Case 3, except that it assumes that all liquid feed reaches the PE particles before evaporation, i.e.  $C_f = 1.0$  (vs.  $C_f = 0.0$  for Case 1). Case 1 is a dry feed with zero liquid in the feed. It is shown from Figure 15 that the particle temperature rise difference between Cases 1, 2 and 3 is negligible, while the difference between Case 4 and the rest is only 0.5 °C indicating that even if all the liquid is assumed to reach the PE particles before vaporization, it would result in reducing the surface temperature of the particle by only 0.5 °C vs. a dry feed case. It should be emphasized, however, that the addition of liquid HC has a pronounced effect on controlling the reactor bulk gas temperature as most of this liquid is evaporated to the gaseous phase before it reaches the polymer particles, hence the bulk gas temperature does not increase by the liberated heat of polymerization. It could also have the effect of moderating particle fragmentation through different mechanisms such as absorption of a small fraction into the polymer particle, which is not discussed here.

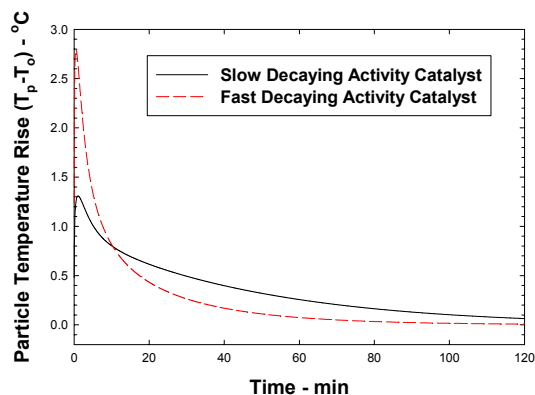


Figure 9: Polymer particle surface temperature above reactor mean bulk temperature.

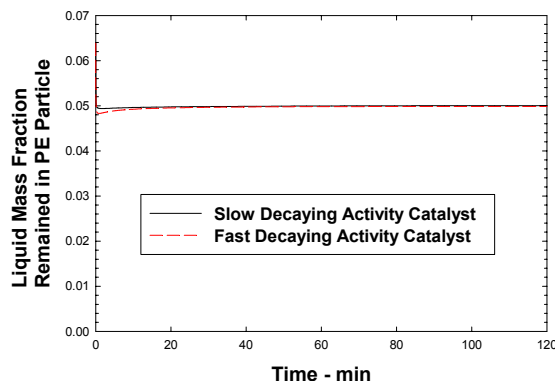


Figure 11: Liquid fraction remained or diffused in the polymer particle during the 2-hour polymerization in the generic reactor.

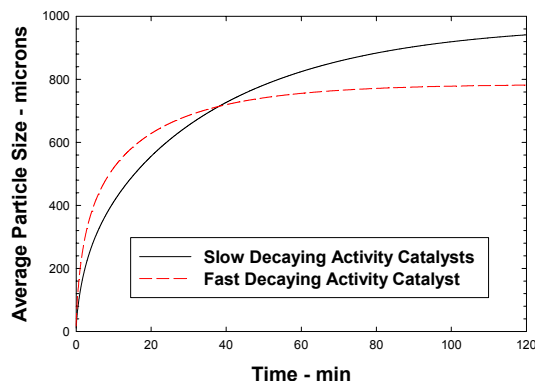


Figure 10: Average particle size during 2-hour polymerization in the generic reactor.

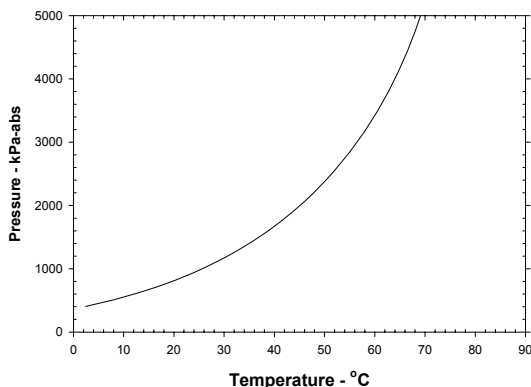


Figure 12: Dew point plot of the total feed mixture obtained using Peng-Robinson equation of state.

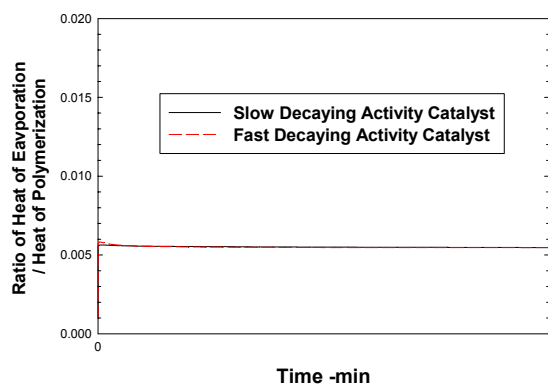


Figure 13: Fraction of polymerization heat dissipated by liquid evaporation.

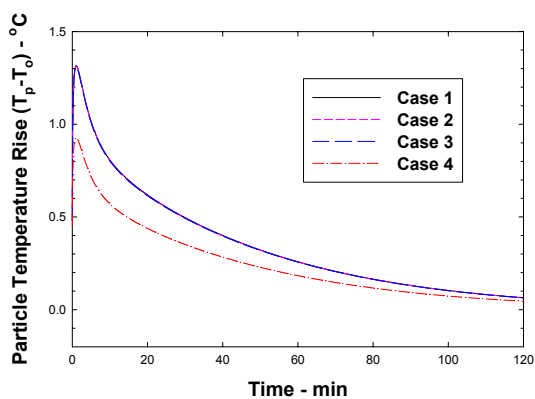


Figure 15: Results of the four cases in Table 1 showing the effect of liquid feed on particle temperature.

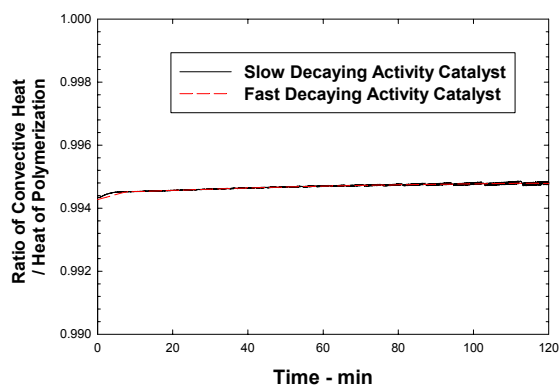


Figure 14: Fraction of polymerization heat dissipated by convection to bulk gas.

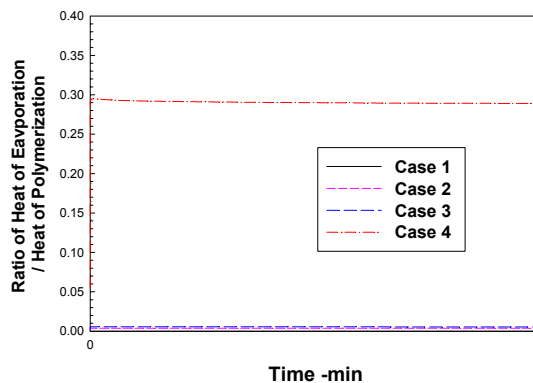


Figure 16: Results of the four cases in Table 1 showing the ratio of heat of evaporation to heat of polymerization.

### Three-Dimensional CFD Analysis:

Results of the full CFD simulation conducted on the generic reactor will now be presented. This is a full transient, three-dimensional analysis to reveal the temporal and spatial variations in the local gas and solid particle temperature within the fluidized bed. Hence, the effect of local hot spots due to stagnant flow and/or relatively cool gas bubbles passing through the bed on particle temperature are captured rather than assuming a uniform gas temperature through the vessel as was the case for the one-dimensional analysis.

The CFD simulations were performed using Fluent v6.1.23 [10], a commercial CFD package. The multi-fluid granular Eulerian approach [11] was used to model the motion of the gas and solid polymer particles in the turbulent, bubbling fluidized bed. Aggregation and fragmentation were neglected in these simulations, as was the actual growth of the particles because the polymerization takes place over a relatively long time scale compared to the hydrodynamics of the fluidized bed. Instead, the measured particle size distribution (PSD) was represented by finite number of discrete solid-phases each with a characteristic particle diameter. The actual number of solid phases was a tradeoff between using a reasonable number of bins to adequately represent the PSD in the reactor and the CPU time required to conduct the simulations. The heat generation due to polymerization was modeled in an analogous manner as the previous 1-D analysis. The heat generated for a given discrete particle size was

determined from the kinetic profile according to Equation (10). The convective heat transfer between the gas and the particle surface was computed locally in each computational cell via Gunn's correlation, Eqn. (18). The heat transfer resistance inside the polymer particles, i.e. polymer-side heat-transfer, was an order magnitude lower than the resistance due to convective heat transfer, and hence was neglected. Further details of the multi-fluid granular Eulerian model, including the constitutive relationships for the solid phases, gas-solid drag formulation and solid-solid interaction, are presented in Reference [11].

The predicted static temperature of the gas phase at an arbitrary instant in time is illustrated in Fig. 17, where the static temperature contours for the gas are plotted on a vertical slice plane passing through the centerline of the reactor. An interesting observation is that the gas heats up rapidly just after it enters the fluidized bed (bottom of the reactor), and then slowly heats up as the gas moves vertical upwards through the bed. The deviation of the solid phase temperature from the local gas temperature is shown in Figures 18 and 19 for the very small and very large polymer particles, respectively. The largest temperature differences are predicted near the bottom of the bed where the cool gas enters. Away from the bottom, the difference between the solid-phases and gas-phase temperature is very small; less than  $0.25^{\circ}\text{C}$  for the very small particles and less than  $0.5^{\circ}\text{C}$  for the very large polymer particles. This is consistent in magnitude with the 1-D results and also with the CFD results for a 2-D bubbling fluidized bed by Fan et al. [8].

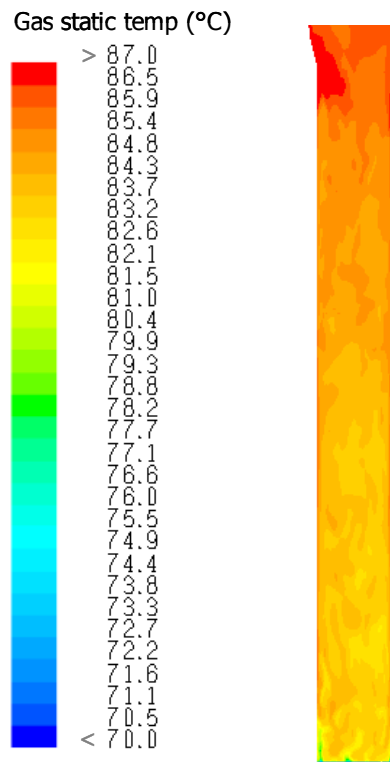


**Figure 17: Contours of gas static temperature plotted on a vertical slice plane through the generic reactor.**

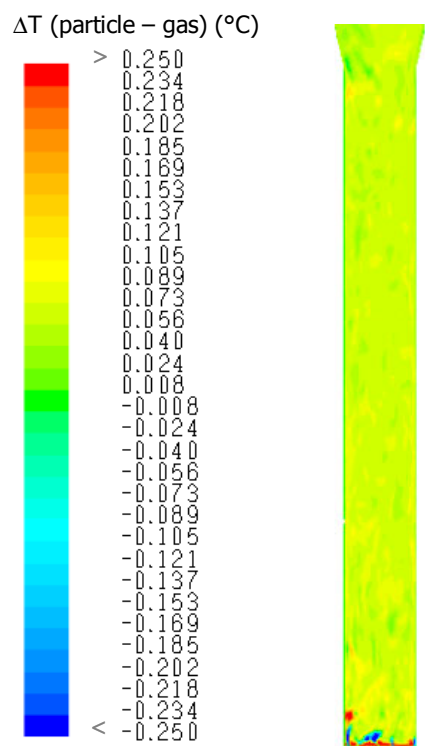


**Figure 18: Contours of temperature difference ( $\Delta T$ ) between small polymer particles and the gas phase plotted on a vertical slice plane through the generic reactor.**

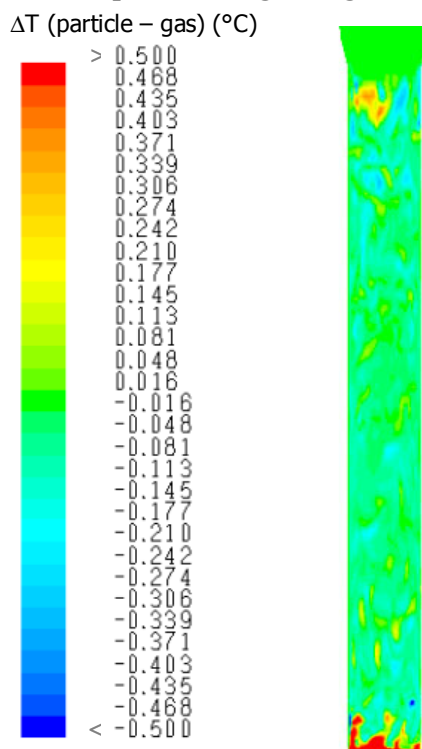


**Figure 19: Contours of temperature difference ( $\Delta T$ ) between large polymer particles and the gas phase plotted on a vertical slice plane through the generic reactor.**

## 6.0 CONCLUSIONS

Theoretically, the capacity limit of a polyethylene gas-phase fluidized-bed reactor is determined by the activity of the catalyst and the ability to remove heat of polymerization from the reactor. When catalyst is not the limiting factor, the addition of liquid HC provides one way to remove heat of polymerization from the reactor. At the same time however, the polymer particles formed become larger and more uniform in size. A possibility is that most of this improvement could arise from a change in the mechanism of heat removal from the polymer particles. Employing experimentation to examine this mechanism seems to be difficult and impractical. Instead, simulation and modeling was used in the present investigation.

From all of the foregoing results, it appears that the addition of liquid HC does not seem to alter the mechanism of heat removal from the polymer particles. It was found that the primary mechanism of heat removal heat from the particles is by means of convective heat transfer to the bulk gas, which amounts to 99.5% removal of the total heat of polymerization. Only 0.5% of the heat of polymerization is removed by *evaporation* of the liquid feed *from the polymer particles*. However, the liquid HC does in fact contribute, in a very significant way, to controlling the reactor overall bulk gas temperature. In the absence of liquid HC feed, the bulk gas temperature will rise depending on the polymer production rate and the heat removal capacity of the external cooler. The liquid HC appears to absorb the heat of polymerization within the fluidized bed reactor (through evaporation) and then releases this heat in the external cooler through condensation without significantly increasing the number of recycling passes. This helps in maintaining the reactor bulk gas temperature at high production rates without sacrificing the conversion rate. An important conclusion arrived at in the present study is the fact that the PE particle temperature is only a couple of degrees Celsius above the bed bulk temperature due the high convective heat transfer coefficient between the PE particles and the bulk gas. This finding is consistent with Yannoulakis et al [2] where the temperature rise was modeled as function of particle size. Liquid feed vs. no liquid feed has little bearing on the temperature rise of the particle above the bed bulk gas temperature. Therefore, the present study reveals that the poorer particle morphology (shown in Figure 1-b) is not due to excessive particle temperature excursions in the absence of liquid HC. It appears that the good resin morphology in the presence of liquid HC is due to a different mechanism, e.g., swelling of polymer particles and change in its elastic characteristics. A swelled polymer particle with higher elasticity appears to reduce particle fragmentation and provide more controlled particle growth.

Finally, the above model assumed that the monomer diffusion into the particle is instantaneous and uniform. It is recommended that an appropriate diffusion model be incorporated into the solution scheme, which may provide more accurate prediction of the particle surface temperature.

## 7.0 ACKNOWLEDGMENT

The authors wish to thank Dr. Umesh Karnik, Dr. John Henderson, Dr. Mark Kelly, Dr. James Muir and Mr. Eric Clavelle of NOVA Chemicals Corporation for valuable discussion during the course of this study. Permission to publish this paper by NOVA Chemicals Corp. is hereby acknowledged.



## 8.0 REFERENCES

1. Pater, J.T.M., Wiekert, G. and Van Swaaij, W.P.M.: "Optical and Infrared Imaging of Growing Polyolefin Particles", *AICHE Journal*, 49, p. 450, (2003).
2. Yannoulakis, H., Yiagopoulos, A. and Kiparissides C.: "Recent Developments in Particle Size Distribution Modeling of Fluidized-bed Olefin Polymerization Reactors", *Chemical Engineering Sciences*, 56 (2001), 917-925.
3. McKenna, T.F., Dupuy, J. and Sptiz, R.: "Modeling of Transfer Phenomena on Heterogeneous Ziegler Catalysts: Differences Between Theory and Experiment in Olefin Polymerization (an Introduction)", *J. Applied Polymer Science*, vol. 57, 371-384, 1995.
4. McKenna, T.F., Cokljat, D., Sptiz, R. and Schweich, D.: "Modeling of Heat and Mass Transfer During the Polymerization of Olefins on Heterogeneous Ziegler Catalysts", *Catalysis Today*, vol 48, 101-108, 1999.
5. Ranz, W.E. and Marshall, W.R.: "Evaporation from drops", *Chem. Eng. Prog.*, 48(30, 141 (Part I) and 48(4), 173 (Part II), 1952.
6. Kiel, J.H.A., Prins, W. and Van Swaaij, W.P.M.: "Modeling of non-catalytic reactions in a gas-solid trickle flow reactor: dry, regenerative fuel gas de-sulphurisation using a silica-supported copper oxide sorbent", *Chem. Eng. Science*, 47(17/18), 4271, 1992.
7. Gunn, D.J.: "Transfer of Heat or Mass to Particles in Fluidized Beds", *Int. J. Heat and Mass Transfer*, Vol. 21, pp. 467-476, 1978.
8. Fan, R., Marchisio, D. L. and Fox, R. O. "CFD simulation of poly-disperse fluidized bed polymerization reactors, submitted to AIChE Symposium Series (2003).
9. Holman, J.P.: *Heat Transfer*, Seventh Edition, McGraw-Hill, 1990.
10. FLUENT 6.1 User's Guide, Lebanon, 22.4 Eulerian Model, Fluent Inc, 2003.
11. Syamlal, M., Rogers, W. & O'Brien, T.J., *MFIX Documentation: Theory Guide*, U.S. Department of Energy, DOE/METC-94/1004, 1993.